A STUDY OF THE SHORT FATIGUE CRACK GROWTH CHARACTERISTICS OF INCONEL 625 BY MODIFICATION AND APPLICATION OF A SHORT FATIGUE CRACK GROWTH MODEL

By

ROBERT GLEN STONE

Bachelor of Science
in Mechaninal Engineering

Oklahoma State University

Stillwater, Oklahoma

1987

Submitted to the Faculty of the
Graduate College of the
Oklahoma State University
in partial fulfillment of
the requirements for
the Degree of
MASTER OF SCIENCE
May, 1989

A STUDY OF THE SHORT FATIGUE CRACK GROWTH CHARACTERISTICS OF INCONEL 625 BY MODIFICATION AND APPLICATION OF A SHORT FATIGUE CRACK GROWTH MODEL

Thesis Approved:

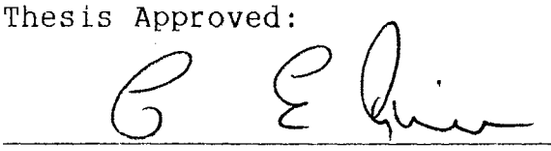

Thesis Advisor

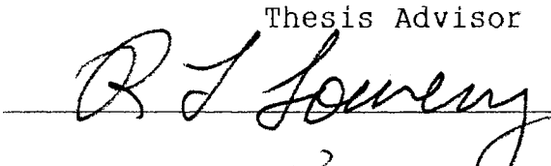

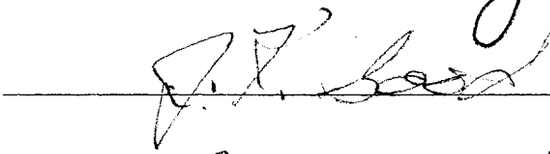

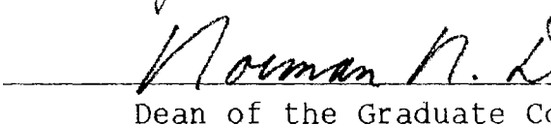

Dean of the Graduate College

ACKNOWLEDGMENTS

I wish to express my sincere appreciation to Dr. C. E. Price for his guidance, encouragement, and patience throughout my graduate program. I would also like to thank Dr. Delcie Durham for her support and suggestions. Thanks also go to Dr. J. K. Good and Dr. R. L. Lowery for serving on my graduate committee.

I owe many thanks to my mother, Ilona Stone (the eagle-eyed editor), and my father, Paul Stone for their support, both moral and occasionally financial, throughout my education. The generous support of my wife Tammy helped me through many a long night in the final stages of this study. Friends like Danny, Paul, Rachael, and Steve provided me with support, encouragement, and a helping hand. To all of these people I extend my sincere gratitude.

TABLE OF CONTENTS

LIST OF TABLES

LIST OF FIGURES

CHAPTER I

AN OVERVIEW OF FATIGUE

Fatigue is the failure of a component subjected to alternating stresses, often below the yield stress of the material in use. This failure is in the form of the initialization and propagation of a crack in the component. For years, fatigue has been recognized as a problem. First, fatigue is responsible for the delayed failure in components subjected to loads which would not cause failure under static conditions. Second, once the problem was recognized, techniques had to be developed to deal with fatigue in the design stage in order to prevent component failure. Third, in addition to modifying design techniques, it was soon realized that fatigue resistant materials were needed to reduce cumbersome designs.

Traditionally, fatigue has been dealt with in the design phase in an empirical fashion. This is obviously the case in Shigley's Mechanical Engineering Design in which design calculations utilize empirical factors to account for conditions affecting the fatigue life, such as surface roughness, size, reliability, temperature, stress concentration, and other miscellaneous

conditions. This approach is continued in the most recent edition of Shigley's text (Shigley and Mishke, 1988). This method is effective but can easily lead to over-designed products. This design philosophy is partly a result of a lack of knowledge of the fatigue process.

More recently, designers have concluded that more efficient product design could take place if fatigue considerations were dealt with in a less empirical manner. This would require a much more detailed knowledge of the fatigue process. As was stated above, fatigue failure may be broken into crack initiation and propagation. Either of these may dominate during component life; however, the propagation of the fatigue crack often takes place over a much greater portion of the component life than the initiation. Research has produced some accurate models for crack growth; however the initiation is not yet well defined. With this greater knowledge, designers could predict the useful life of a component based on assumed loadings. The United States Air Force has adopted this design philosophy (Gallagher et al, 1984). However, one main problem remains. This technique assumes the presence of pre-existing flaws in the components prior to use. There are two main reasons for this assumption. The first is that inspection techniques are not fool-proof. For any specified inspection technique, there is a lower limit to its flaw detection ability. Therefore, to be prudent, one must assume the existence of flaws just smaller than the smallest flaw

detectable by the specified inspection technique. The second reason is less obvious and has already been mentioned. Although the fatigue crack growth characteristics have been well modeled, the initiation of fatigue cracks is not completely understood. Therefore, to avoid designing for the initiation of fatigue cracks, the accepted technique is simply to assume that very small cracks already exist in the new part.

Fatigue crack growth can be divided into three stages. Stage I involves the growth of very short cracks immediately following initiation; Stage II involves the stable growth of long cracks; and Stage III involves the unstable crack growth to failure. The second and third of these stages have been the subject of considerable study and are well understood. Accurate models for crack growth in these stages have been developed and supported by countless experiments. The models in these stages assume that the material's microstructure has no effect on the crack growth. In other words, Stage II and Stage III crack growth are macroscopic phenomena rather than microscopic.

However, it is not prudent to assume that this holds true for short cracks, which have a length on the order of one grain diameter. In fact, Stage I crack growth behavior is very different from either Stage II or Stage III crack growth. One must recognize that, for cracks of this small size, the grain size and

orientation must play a critical role in the crack growth characteristics. This concept is what separates Stage I crack growth from other crack growth modes. This idea has only recently gained significant attention. Therefore, very few Stage I crack growth models have been developed.

Fatigue has also been dealt with in the development of materials. Many materials have been developed specifically as a result of the need for fatigue resistance. Initial development of corrosion resistant alloys was centered, primarily, on corrosion resistance and, secondarily, on strength. It was soon obvious that fatigue resistance was needed in these alloys. As a result of this research, the Inconel alloys, and more specifically Inconel 625 (NO6625), were developed. Inconel 625 is often selected when both corrosion- and fatigue-resistance are needed. Therefore, any efforts to understand better the fatigue process and how it relates to this material are welcomed. That makes Inconel 625 an ideal candidate for fatigue research.

This thesis will examine one of the existing Stage I crack growth models, comment on its problems, and propose modifications which will improve the model. These modifications will be justified by comparing the model to experimental data. Because of the material selected for this study, the information generated should be both useful and relevant.

CHAPTER II

TESTING AND MEASUREMENT PROCEDURES

Specimen Preparation

The material selected for testing was Inconel 625. The specific heat used was NX 76A6AS having a chemical composition by weight percent as follows: 61.38 Ni, 22.02 Cr, 9.27 Mo, 3.63 Cb and Ta, 2.52 Fe, 0.26 Ti, 0.22 Al, 0.16 Si, 0.10 S, 0.02 C, 0.02 Mn, and 0.02 Cu. The material was supplied in sheet form with a 0.062 inch thickness in the cold rolled annealed condition with a grain size of approximately 25 μm and a hardness of HRB 96. Microstructural examination of the material showed substantial stringers. For this reason, although the material had been annealed, it was not isotropic. Therefore, both L-T and T-L specimens were machined for testing. Specimens had nominal dimensions of 0.5 inches wide x 5 inches long x 0.062 inches thick. To study the microstructural aspects of short fatigue crack propagation, the grain size as supplied was much too small. The grain size was enlarged to approximately 100 μm by soaking the specimens at 1200°C for one hour in an Argon environment. The resulting hardness was HRB 86. A notch was cut into one side of the specimen using a low speed diamond

saw. This notch, being the primary stress concentration, served as the initiation point for any fatigue cracks which would develop. The notch depth was approximately 0.04 inches. The specimen geometry with nominal dimensions is shown in Figure 1. Examination of the notch root showed it to be nearly round. To simplify measurement of the notch root radius, the notch root was assumed to be round. Therefore the notch root radius was taken to be half the notch width of approximately 0.016 inches. In order to protect the surface of the specimens during in-test inspection, only one side was used for measurement purposes. For each specimen, this side was specified prior to testing and only this side was polished for inspection. These surfaces were mechanically polished through 5 micron alumina using flooded wheels at low speeds and minimal pressure for the final stages. To help prevent corner cracks from forming in the opposite side, the reverse side was ground smooth using 600 grit grinding paper. The specimens were now ready for testing.

Testing Procedure

The specimens were individually subjected to alternate tensile loading of such magnitude as to provide a life of approximately 250,000 cycles. An MTS testing machine was used to perform the tests under constant load range using a sinusoidal loading wave form at 40 Hz. Specimen lives near the target were obtained

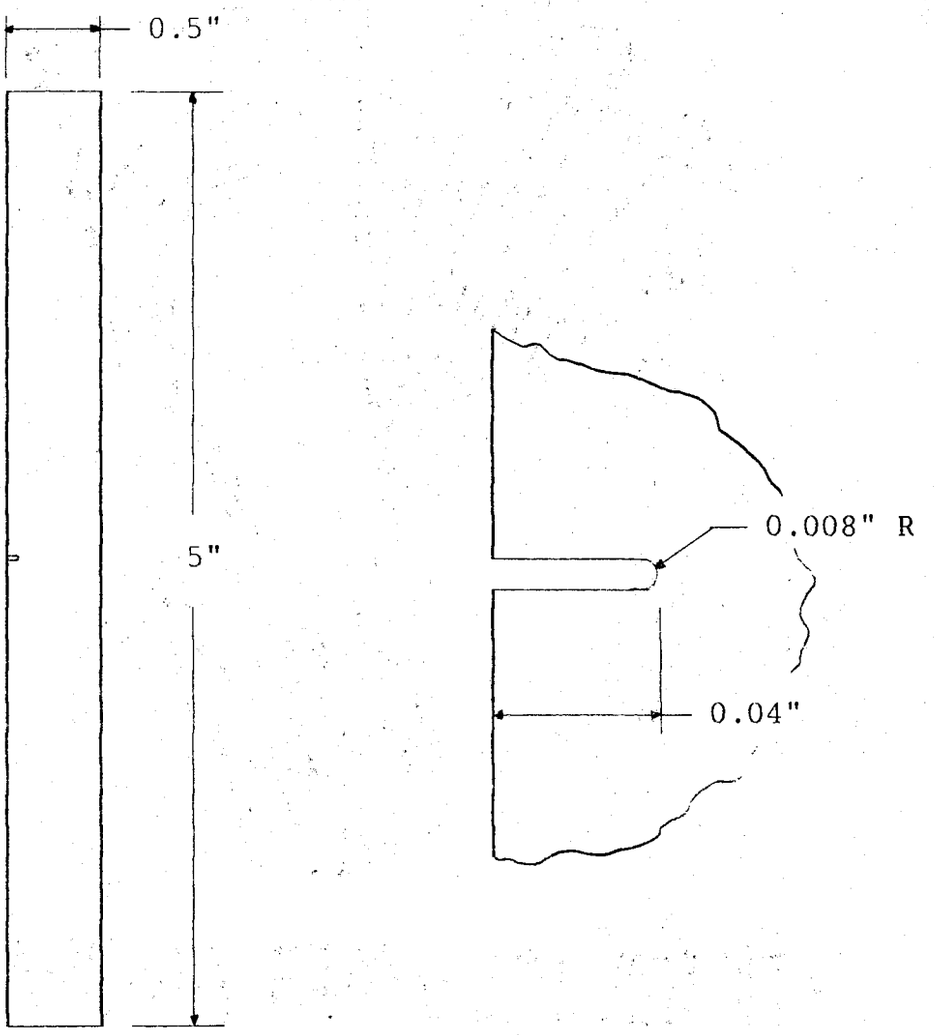

Figure 1. Specimen Geometry

when the applied loads varied from 725 to 1275 lb. This loading was selected after preliminary testing primarily out of convenience since it repeatedly provided specimen lives near the target life. The target life of 250,000 cycles was selected because it put the specimens in the high cycle fatigue regime with sufficient life as to simplify the distinction between crack growth stages and with a life short enough that specimens could be tested to failure without requiring excessive testing time.

Measurement Technique

Periodically, the specimen being tested was removed from the apparatus, the number of loading cycles noted, and then examined under Nomarsky interferometry. This high resolution technique would allow the observation of slip prior to cracking in addition to easy measurement of the cracks themselves. Cracks were photographed through the Nomarsky interferometer using color slide film and the magnification of each photograph was noted. Photographs were also taken of a reference scale at various magnifications. A set of rulers was made using the projections of this reference scale. These rulers were used to measure the projection of the cracks. Construction of a new set of rulers was necessary each time a measurement session began since the positioning of the projector could not be accurately duplicated day to day.

By comparison to continuous tests, if conducted with care, the interrupted loading was determined not to have any discernable effects on the fatigue life of the specimens.

CHAPTER III

IMPROVEMENT OF AN EXISTING SHORT CRACK GROWTH MODEL

Short Crack Growth Model

Researchers have recognized short crack propagation as a unique problem for some time; however, as was previously mentioned, very few models of short fatigue crack growth have been developed. Much of the work done to this point is centered on modification of linear elastic fracture mechanics (LEFM) so as to incorporate short crack growth. Since microstructural effects are ignored by LEFM and short crack growth apparently is dominated by microstructural effects, this approach seems illogical. One of the more elegant models that have been developed that breaks this link to LEFM is that of Hobson (Hobson, 1982). His equation describing short crack growth is:

$$\frac{da}{dN} = C(d-a)^{1-\alpha}a^{\alpha}. \qquad (1)$$

This model assumes that crack arrest will occur when the crack length, a, reaches a length corresponding to the termination of short crack growth characteristics, d. Strictly speaking, d is the distance between microstructural barriers which inhibit crack growth. This is often taken to

be one grain diameter. The model also accounts for two factors judged critical to short crack growth. Specifically, these are the slip band plastic zone, (d-a), and the fatigue crack length, a.

Crack Data Collection

Although Hobson's model seems rather simple, its application can be intricate. Even Hobson showed that use of this model often requires some questionable assumptions (Hobson, 1986). In his 1986 paper, he deals only with surface cracks on cylindrical specimens. This presents a problem. The crack front shape is not determined. Therefore, very little is actually known about the crack. Modeling the growth of the crack front would provide a much more useful result. This problem centers around the specimen geometry selected. For this type of analysis, a cylindrical specimen would not provide the most desirable information. Choosing a specimen geometry such that surface crack data is more relevant is a necessity. For this reason, a flat notched specimen was selected for this analysis. The cracks were assumed to be through-thickness. This assumption gave the surface crack data taken greater significance. The assumption would hold provided no corner cracking occurred. Scanning electron microscope inspection of failed specimens showed no evidence of corner cracking. Therefore, surface crack data could be used to provide an analysis with results that are much more informative.

Calculation of Parameter d

Hobson's technique for calculating the parameter d is briefly described. The fatigue crack is measured at certain points during the testing. At these points the corresponding number of loading cycles is noted. This set of data is then used to calculate a crack growth rate over each interval using the secant method. It is assumed that this average crack growth rate corresponds to a crack length midway between the data points. The points generated are then plotted. During Stage I crack growth, the growth rate continually decreases. This is supported by experimental data and is a key assumption in short crack growth models. Therefore, the sequential points which show a continual decrease in growth rate are then approximated by a line using the least squares technique. The parameter d is taken to be the intersection of this line with the abscissa. This would correspond to a crack growth rate of zero when the crack length is equal to d. A schematic representation of this technique is given in Figure 2.

Hobson's technique described above has much room for improvement. The selection of the secant method of approximating crack growth rate data is a poor one. For even a well-behaved function, secant data is only acceptable as a first-pass approximation. When the crack length approaches d, corresponding to a transition from Stage I to Stage II growth, growth rates are extremely low and there is no indication that the growth function should be well behaved.

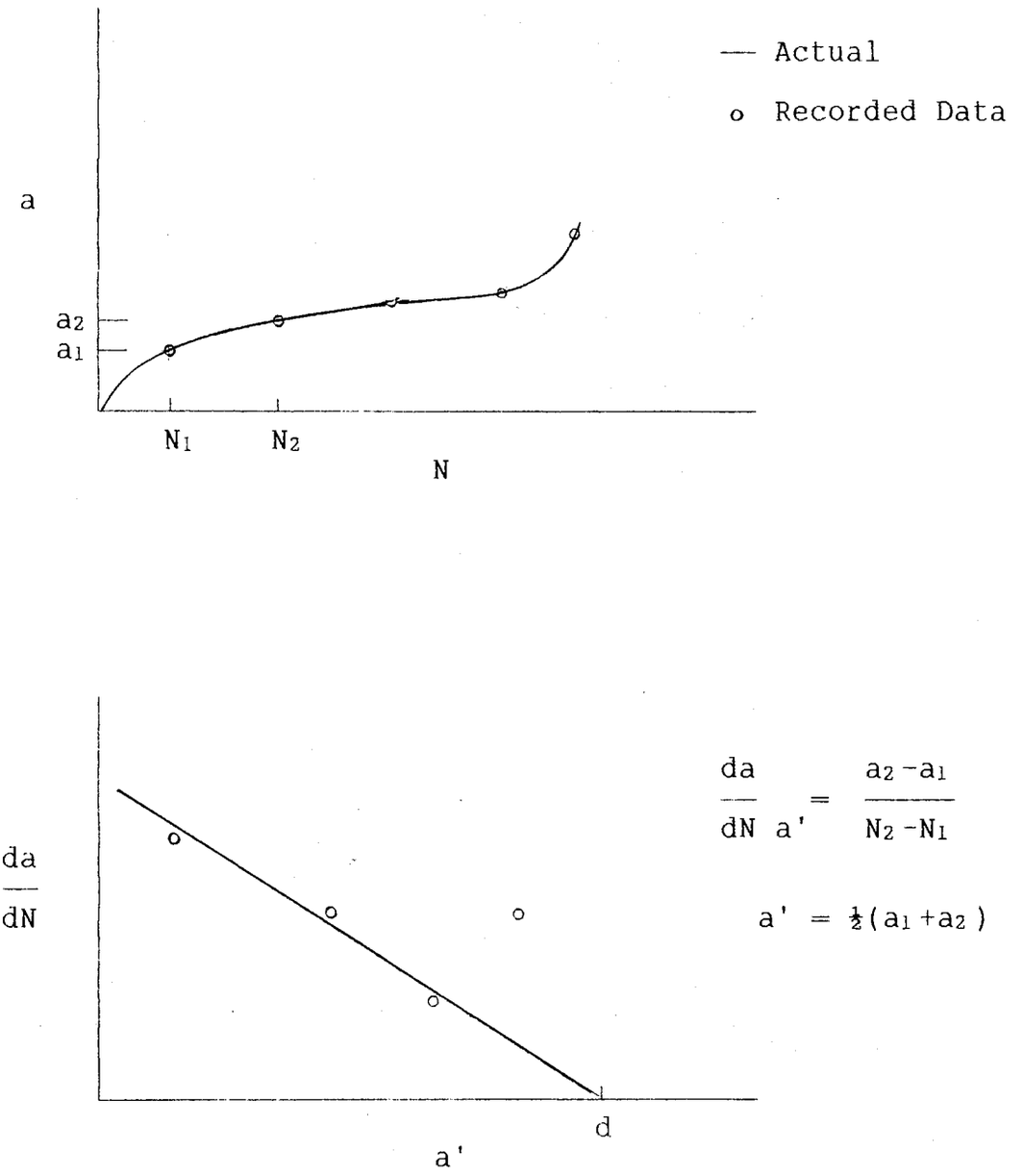

Figure 2. Hobson's Technique for Determining d

Since two distinctly different phenomena play roles in the proximity of this transitional crack length, there is no reason to expect the growth function to be well-behaved. Therefore, it is very likely that secant data calculated using crack lengths very near or, in particular, bounding the d value are susceptible to significant error. These errors would tend to lead to estimates of d larger than the actual value.

This study revised Hobson's technique of applying his short crack growth model in an effort to reduce the errors previously mentioned. This analysis fitted a polynomial of at least fourth order to the first few points of the original crack length data. The points to be used in the fitting were determined after initial examination of the data using secant method approximations of the growth rate. Whenever possible, the points used were the initial point through the ending point of the first range showing an increase in crack growth rate. This polynomial was then differentiated. The resulting polynomial provided an approximation of the crack growth rate as a function of fatigue cycles. This growth rate could be related to the crack length by way of the original polynomial. In most cases, the crack growth rate curve did not cross the abscissa. This was expected since the growth rate approximation was the derivative of a fitted curve. The value of d was taken to be the minima of the growth rate curve. In general, these values were significantly lower than the values calculated by the

technique presented by Hobson. Figure 3 gives a graphic comparison of the two techniques.

Determination of α

Hobson showed in his analysis that, for the particular material he was studying, the parameter α was nearly zero. This was demonstrated by plotting da/dN vs. (d-a) on a log-log scale for various specimens. The resulting plots all had a slope of nearly unity. This meant that the term $(1-\alpha)$ had a value of nearly one. Therefore, α had a value very near zero. The assumption that this parameter had a value of zero significantly simplified the remaining analysis. However, his 1986 study was based on steel alloys. Duplication of Hobson's technique showed that the parameter α did not have a value near zero for the material in this study. Therefore, it was necessary to develop a technique of determining the value of α.

Taking the logarithm of both sides of (1) gives:

$$\ln\left(\frac{da}{dN}\right) = \ln(C) + (1-\alpha)\ln(d-a) + (\alpha)\ln(a). \qquad (2)$$

At this point in the analysis, a function has been developed which approximates the growth rate as a function of crack length and a value has been determined for the parameter d. With the equation in the above form, it is easy to see that the term involving the factor C is merely an offsetting term. With this information, a method of determining α is quickly developed.

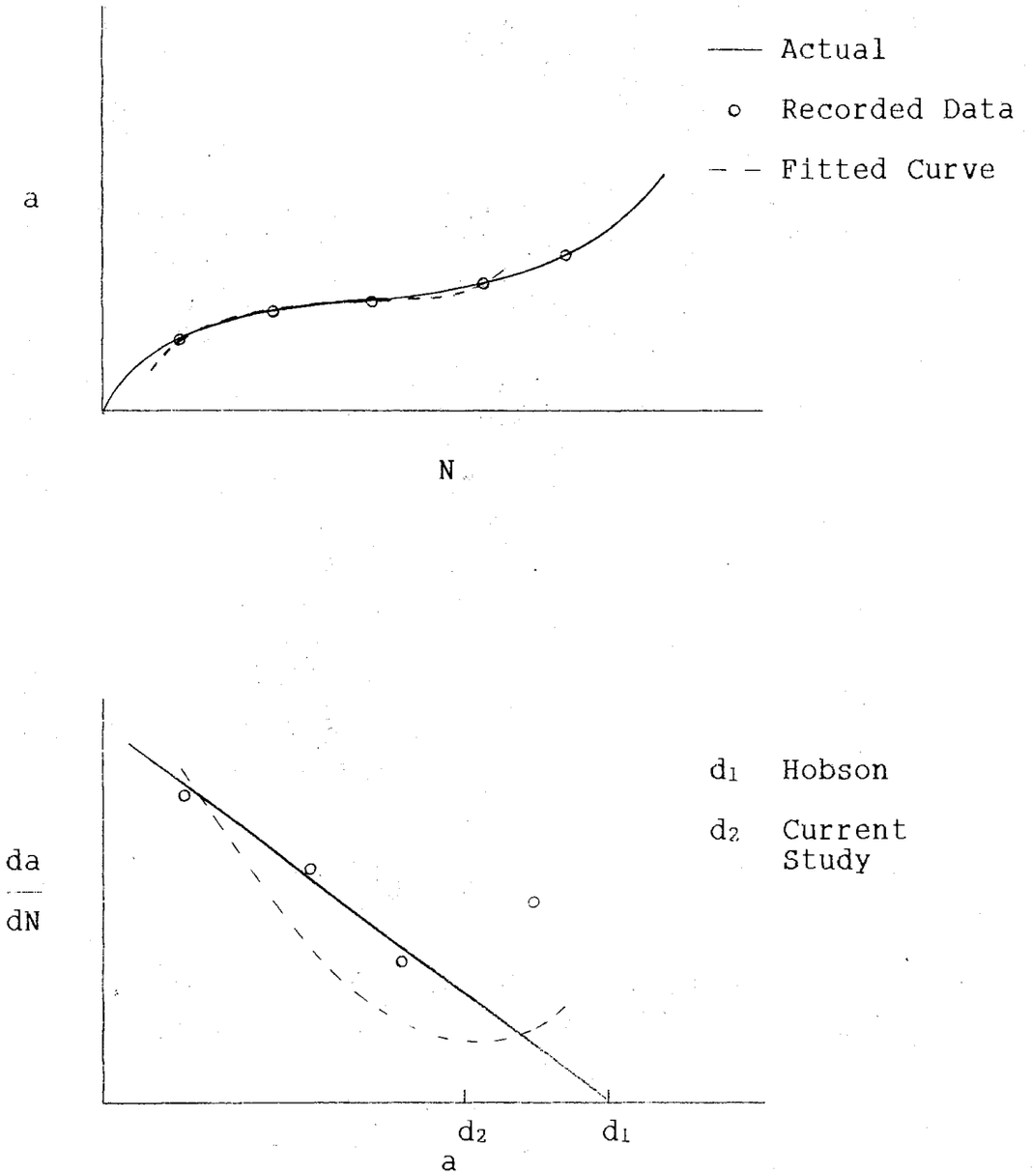

Figure 3. Comparison of Techniques for Determining d

Data points of the crack growth rate at various crack lengths can be generated using the polynomial previously used to determine the value of d. This is done at twenty equally spaced crack lengths from zero to d. A value of α is then assumed. The first of the data points is used to determine the offset ln(C). For the remaining points the error is determined as follows:

$$\text{Error} = \ln\left(\frac{da}{dN}\right) - \ln(C) - (1-\alpha)\ln(d-a) - (\alpha)\ln(a). \quad (3)$$

These errors were squared to avoid cancellation and summed. The estimation of α was then modified and the process repeated. The value of α was taken to be the value providing the lowest error sum. A Pascal program was written to speed these computations.

Formation of a Functional Relationship for C

Hobson suggests that the parameter C in the crack growth rate model should vary with the applied stress range. Therefore, for all specimens tested under the same loading conditions, the same value of C would apply. Hobson determined the function representing C by the following procedure. The value of C was calculated using the crack growth rate model for each successive pair of data points where $a < d$. For all specimens tested, the values of C were plotted against the stress range on a single plot. The resulting plot showed significant scatter in C for any given

stress range. The function used to represent C was the line given by the 95 per cent confidence intervals at the lowest and highest stress ranges used.

The technique stated above has some problems, the most notable of which is the scatter in the values of C. As a result of the analysis in this study, it is noted that the values of C rise dramatically when the crack length approaches d. Hobson showed that the values of C for a given stress range may vary by as much as three orders of magnitude. One of the primary reasons is that the selected value of d may, in fact, be too large as was discussed previously. It is expected that the crack growth rate will increase after the transition from Stage I growth to Stage II growth. By using a value of d in the calculations which is larger than the actual value, the analysis is attempting to incorporate early Stage II growth. With the term (d-a) decreasing rapidly as the crack length increases, the value of C must increase very rapidly to meet the increasing crack growth rate. In other words, the value of C is very sensitive to small changes in the crack growth rate behavior for crack lengths approaching d. It has been shown that the scatter in C comes primarily from data having crack lengths very near d. It has also been shown that this is precisely the area where results are least reliable. Therefore the selection of the 95 per cent confidence interval is not logical. This gives unreasonably large results for C. A more logical choice would have been to select the mean value

of C at each stress range for use in determining the function representing C. This would have reduced the values of C from Hobson's function by an order of magnitude.

In attempting to improve on the technique of determining a relationship for C, many factors must be examined. First is the selection of a value of d. This topic has been discussed previously and an improved technique has been presented which tends to give values significantly lower than Hobson's technique.

Second is the crack growth rate information. Hobson used the secant technique for his growth rate information which gives rise to two problems. First, the secant technique assumes that the average growth rate value over the selected range applies to the midpoint of the range, which tends to reduce the features of the curve being represented, particularly in areas of discontinuities. It is conceivable that two points might be selected that bound the transition crack length d yet having a midpoint less than d. These phenomena are depicted schematically in Figure 4. This would mean that the crack growth rate specified by the secant technique could incorporate both Stage I and Stage II growth for crack lengths very near d while the information is perceived as Stage I crack growth. This could lead to unreasonably high crack growth rates being used for crack lengths very near d. Second, as has already been discussed, the secant technique, by its nature, does not provide the most accurate information available. A polynomial fitted to

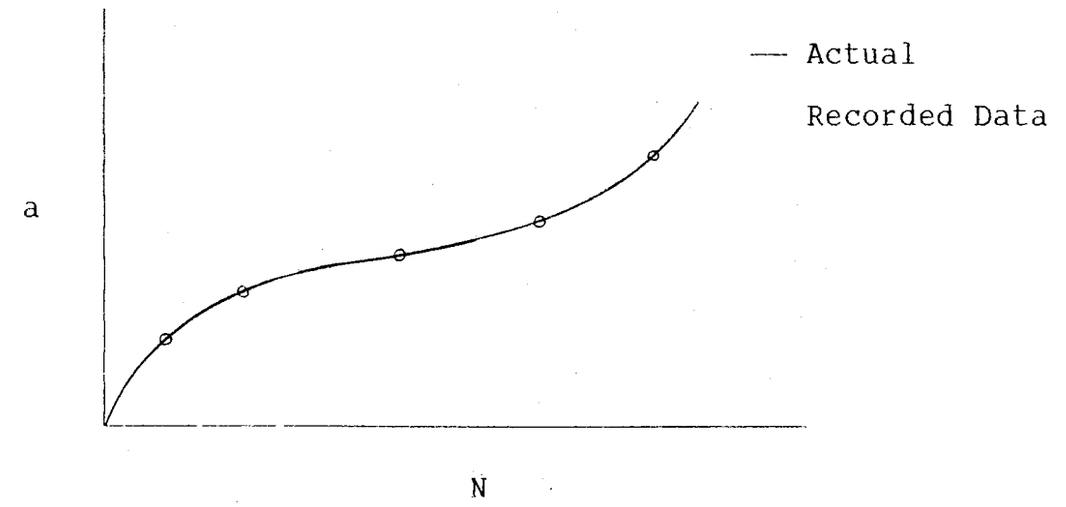

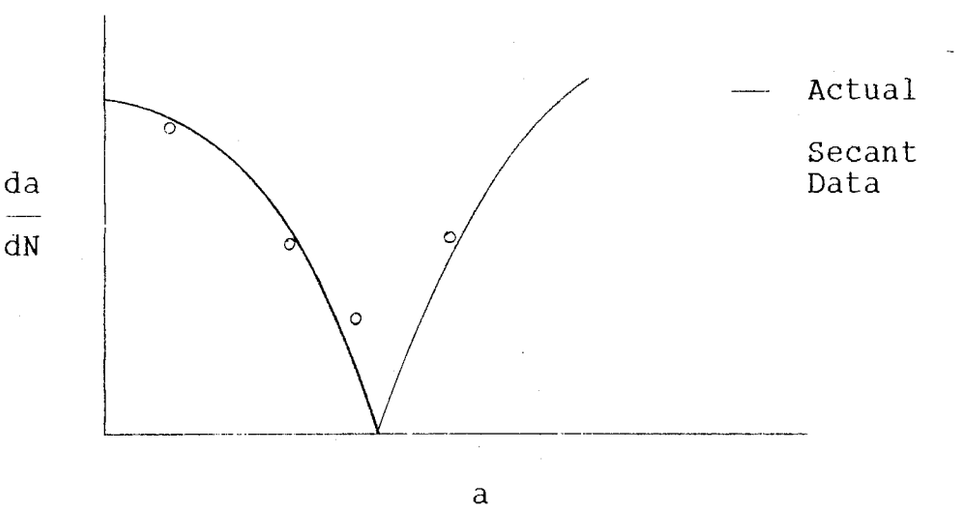

Figure 4. Errors in Secant Method

the crack length data and differentiated will provide more accurate information. As was alluded to previously, this polynomial is not completely accurate. Therefore, crack growth rate information generated by this polynomial for crack lengths near d should be used with great care. The third factor to be examined is the decision that C should vary only with the applied stress range. The specimen loading is a necessary consideration; however, loads seen at the crack front are much more significant than overall specimen loading.

The stress intensity range, ΔK, is generally used in fatigue analyses to account for the effects of both the applied stress range and the specimen geometry, both specimen shape and crack length, in a single factor. Since crack growth behavior varies with both loading and crack length, it is not unreasonable to assume that the stress intensity range is a good parameter to include in the crack growth model. It was decided that, for this study, the parameter C will be allowed to vary as a function of stress intensity range. This means that, in contrast to Hobson's technique, the value of C will be allowed to vary for a given specimen as the fatigue crack length changes. A good selection for the function representing C would then improve the accuracy of the crack growth model.

Before this analysis could continue, the stress intensity range function for the given specimen geometry had to be determined. As was previously stated, the specimen

geometry selected for this study was flat strips with a notch midway along one edge. Radhakrishnan and Mutoh (Radhakrishnan and Mutoh, 1986) showed that an accurate representation for the stress intensity for flat notched specimens with short cracks is as follows:

$$K = \{1 + 1.472\sqrt{(D/\rho)}\}^{1/2} K_{SEN} \qquad (4)$$

where D is the notch depth, ρ is the notch root radius, and K_{SEN} is

$$K_{SEN} = \sigma\sqrt{(\pi a)}(1.12 - 0.23\alpha + 10.55\alpha^2 - 21.72\alpha^3 + 30.39\alpha^4)$$

taking $\alpha = a/W$, W being the specimen width. The stress intensity can easily be converted to a stress intensity range by substituting the stress range for the stress in the above equation defining K_{SEN}. It is interesting to note that the definition for K_{SEN} is the same as the stress intensity factor for an edge-cracked finite width plate as defined by the U.S.A.F. Damage Tolerant Design Handbook (Gallagher et al, 1984).

Using a Pascal program, values of C were calculated for twenty equally spaced crack lengths between zero and d. The values of d and α used in the calculations d were taken to be those determined by the techniques already developed in this study. The function representing da/dN was the polynomial already determined. The resulting values of C were plotted versus the corresponding stress intensity ranges. An example of one of these plots is given in Figure 5.

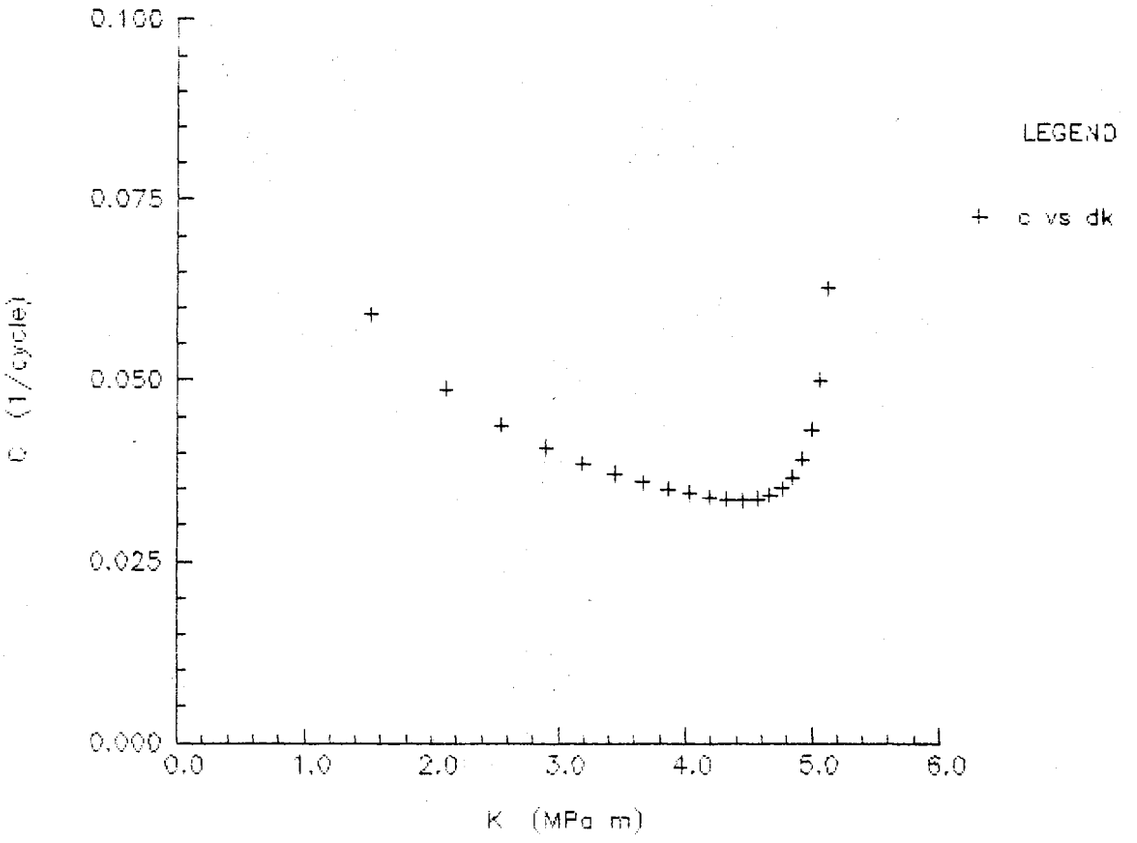

Figure 5. Generated Data for C as a Function of ΔK

The upward turn as ΔK approached ΔK_d, ΔK corresponding to a=d, was quite unexpected. This warranted examination before this result would be accepted. The problem was traced back to the polynomial used to represent da/dN. This polynomial, as was stated previously, usually did not cross the abscissa. Therefore, at a=d the polynomial gave a positive, non-zero value for da/dN. Equation (1) states that the crack growth rate must be zero at a=d. To compensate for this inconsistency, the value of C was forced to approach infinity as (d-a) approached zero such that their product could result in a positive, non-zero result. It can be shown that the error in the resulting value of C is positive and that it increases as a approached d. The more accurate values for C correspond to the smaller values of a. Since the plot of C vs. ΔK is decreasing as a increases in this range, the actual function of C vs. ΔK must also be decreasing. It is unknown how this function actually behaves as a approaches d. Therefore, it is assumed that C behaves linearly in ΔK. The line is taken to be that defined by the first two points generated by the program. This assumption meets both criteria already determined. Specifically, the function is decreasing, at least initially, and the error in the data generated by the computer program increases as a, hence ΔK, increases.

CHAPTER IV

COMPARISON OF RESULTS

Determination of Model Parameters

Of the specimens tested as prescribed above, six were chosen for analysis. The experimental data collected for these specimens is listed in Appendix A. To obtain an overview of the crack growth rate behavior, rough crack growth rate data was then generated using the secant method. This data is supplied in Appendix B. On preliminary examination of the secant data, half of these specimens (specifically, specimens 1, 2, and 6) showed evidence of multiple retardations. It was decided that only the first retardation would be studied in this study.

As is specified by the modified analysis procedure presented in this study, curves were fit to approximate the crack growth rates. A Pascal program was used to perform the curve fits and its output for each specimen is listed in Appendix C. Both Hobson's technique and the technique developed in this study were used to calculate d. In performing the curve fits for some of the specimens, it was not appropriate to use the data points as defined by the guideline given in Chapter III. The secant data showed that, for many of the specimens, the crack growth rate increased

before decreasing. This was not unexpected since the first secant data point was calculated using the first measured data point and a zero crack length prior to loading. Since crack initiation may not occur immediately, this first value is expected to be inaccurately low. For this reason, the data points showing an initial increase in crack growth rate were assumed to be inaccurate and eliminated from the curve fit. The program output in Appendix C indicates the range over which each curve was fit.

The spacing of the data points for specimens 4 and 6 was such that curves could not be fit to the data in such a manner as to provide reasonable results as defined by the prescribed technique. Therefore, for these two specimens, the technique was modified. For specimen 4, a cubic was fit to the experimental data rather than a quartic. The spacing of the data for specimen 6 required the order of the approximation to be reduced further. A quadratic Lagrange polynomial was fitted to the three data points taken from 45,000 cycles to 55,000 cycles. This polynomial is provided in Appendix C in lieu of the program output. The resulting curves were differentiated and the value of d was determined for each of the specimens. these values, along with those calculated by Hobson's technique are listed in Table I.

The values of α were then calculated for the six specimens. As the order of the approximation of the curves decreased, it was expected that more error would be introduced into the approximations which may propagate

TABLE I

COMPARISON OF VALUES OF d FOR SPECIMENS ANALYZED

Specimen Number	d (μm) Hobson	This Study
1	61.4	39.2
2	67.2	42.5
3	76.6	71.6
4	135.3	152.5
5	225.7	214.5
6	101.7	70.7

through the subsequent calculations. This was evident in the value of α calculated for specimen 6; however, it was encouraging to see that, for the most part, the values of α were fairly well grouped. The calculated values are listed in Table II.

Since all specimens saw similar loading, Hobson's technique would provide a single value of C for all specimens. This value was found to be as follows:

$$C = 17.71 * 10^{-5} \text{cycle}^{-1}.$$

Following the prescribed technique, values of C and ΔK were calculated at different crack lengths for each specimen. The results of these calculations are listed in Appendix D. At

TABLE II

VALUES OF α FOR
SPECIMENS ANALYZED

Specimen Number	α
1	0.282
2	0.425
3	0.580
4	0.482
5	0.503
6	0.926

this point, the functional relationship representing C could be obtained. Assuming the function to have the following form:

$$C = c_1 + c_2(\Delta K),$$

the unknown parameters c_1 and c_2 were found for each of the six specimens. These calculations were made taking a in μm and da/dN in μm/cycle. Table III summarizes the results of the calculations. At this point, the crack growth rate model had been fully defined by both Hobson's technique and the technique presented in this study. The two applications of the model could now be compared.

TABLE III

PARAMETERS DEFINING FUNCTIONAL RELATIONSHIP FOR C

Specimen Number	c_1	c_2
1	0.0775	-0.0143
2	0.1005	-0.0296
3	0.3791	-0.0448
4	0.2219	-0.0140
5	0.1715	-0.0096
6	0.3515	-0.0434

Comparison of Results

The results of both techniques were integrated using the Fourth Order Runge-Kutta technique. Since the point of crack initiation was not known, the integration algorithm assumed the cracks to initiate immediately upon loading. Additionally, because of the nature of the Runge-Kutta technique and the nature of the model, it was necessary to assume an initial non-zero crack length. For all specimens, this was taken to be 1 μm. The curves resulting from the integrations were superimposed over the original data. The resulting plots are given in Figures 6 through 11. As was expected, the results showed immediate crack initiation. Since this may not be the actual case, and the actual point

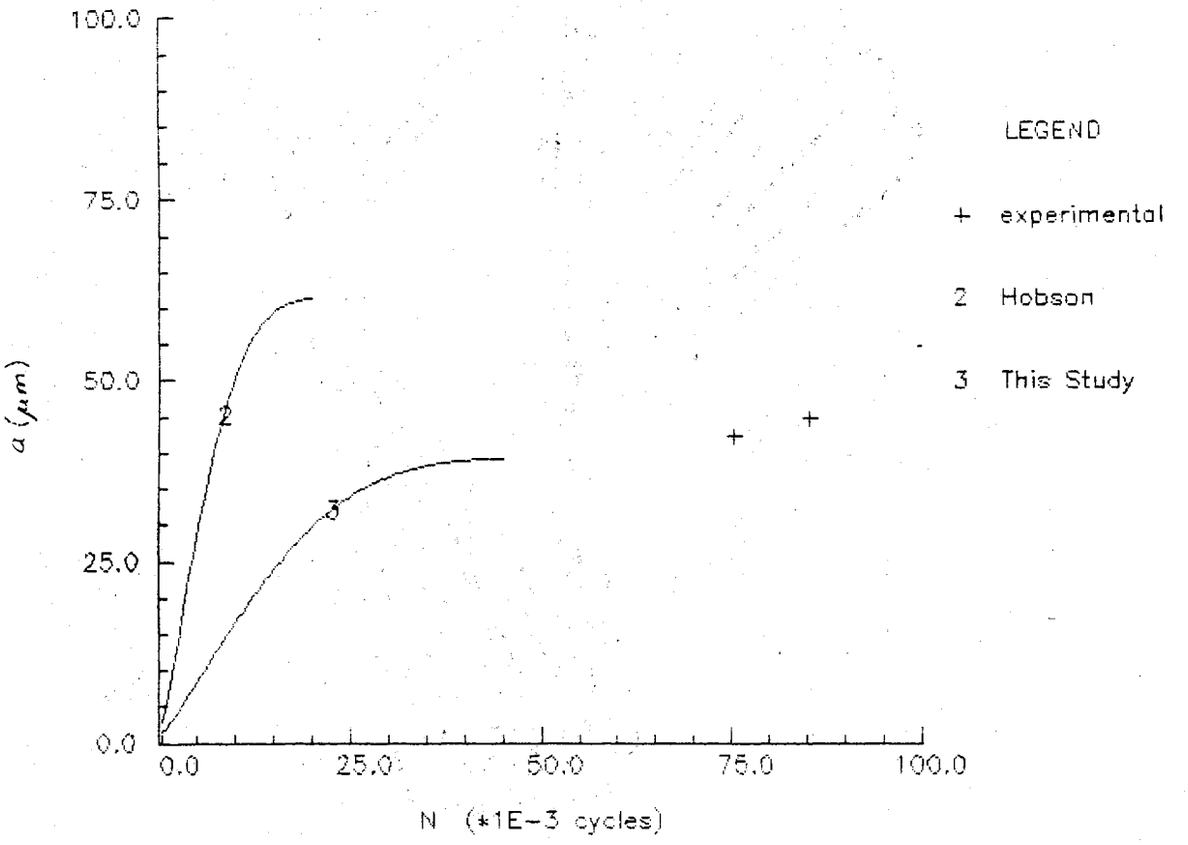

Figure 6. Plot of Model Approximations and Experimental Data for Specimen 1

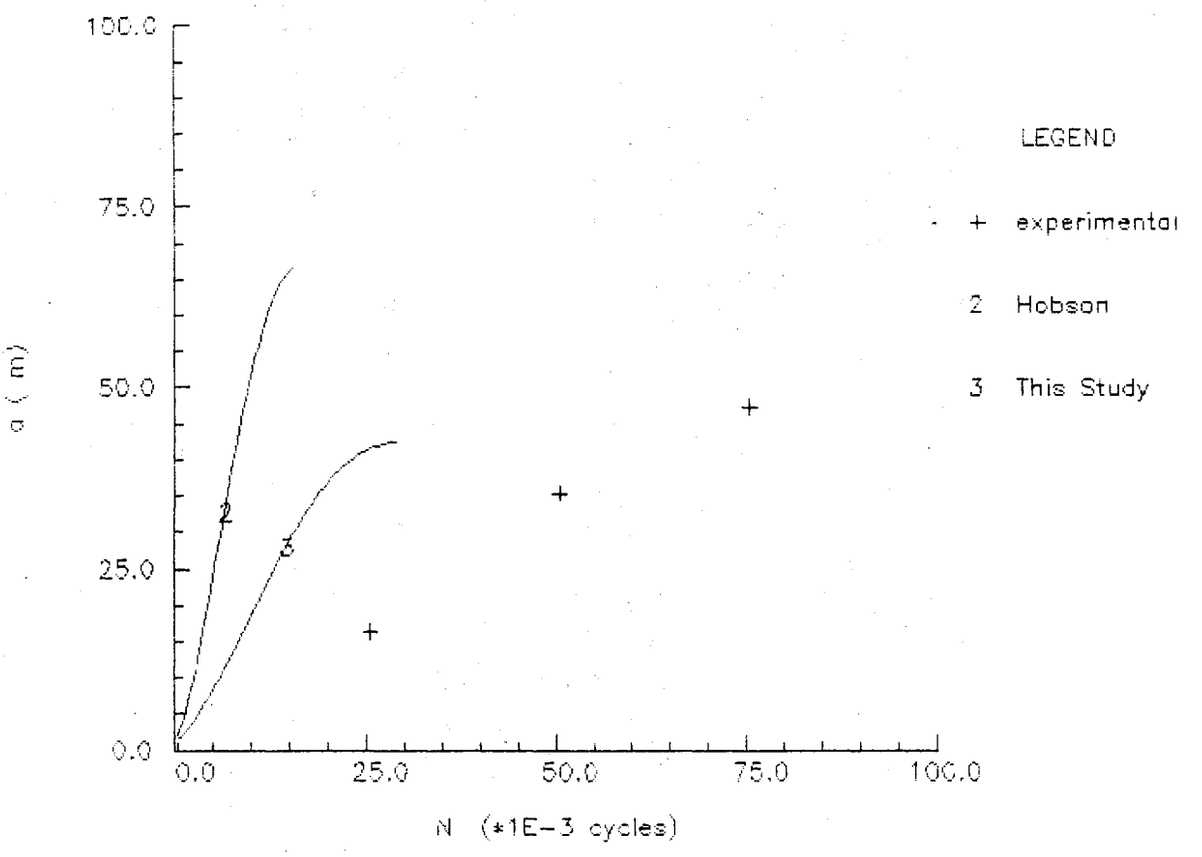

Figure 7. Plot of Model Approximations and Experimental Data for Specimen 2

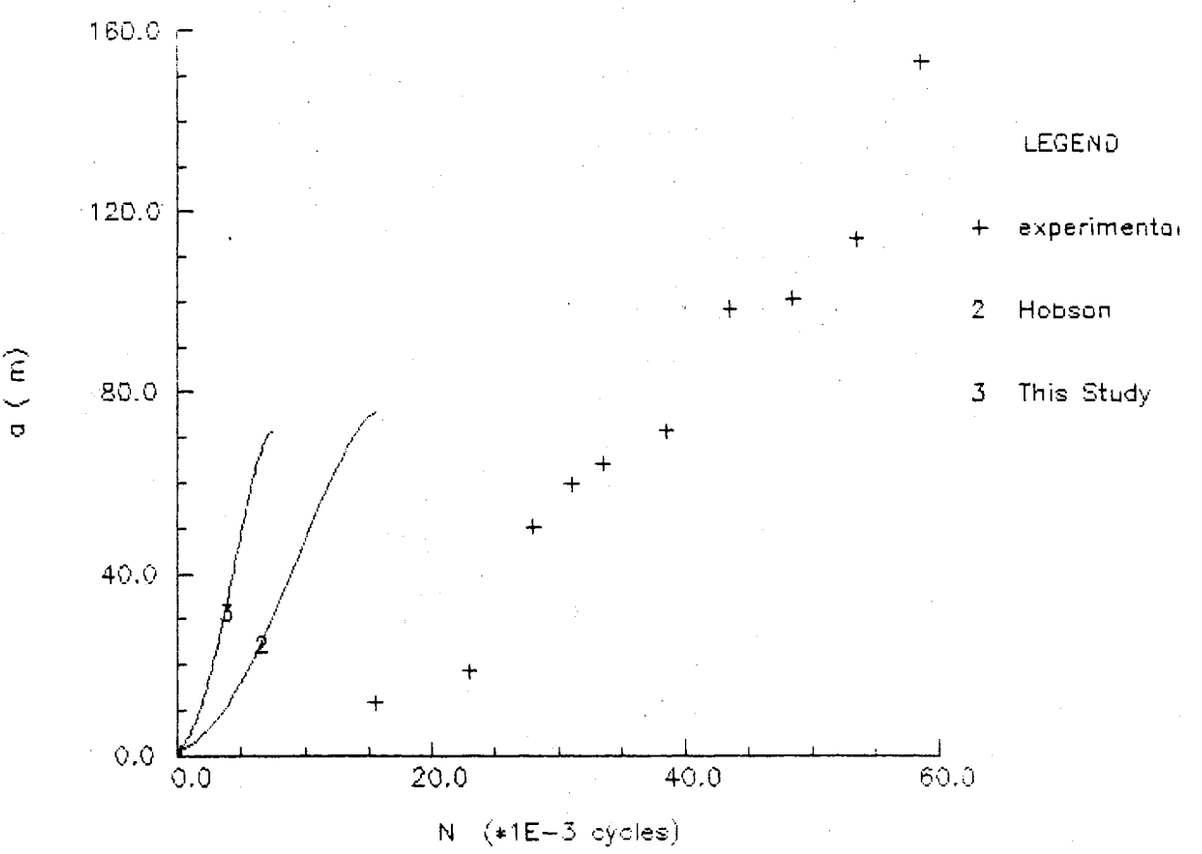

Figure 8. Plot of Model Approximations and Experimental Data for Specimen 3

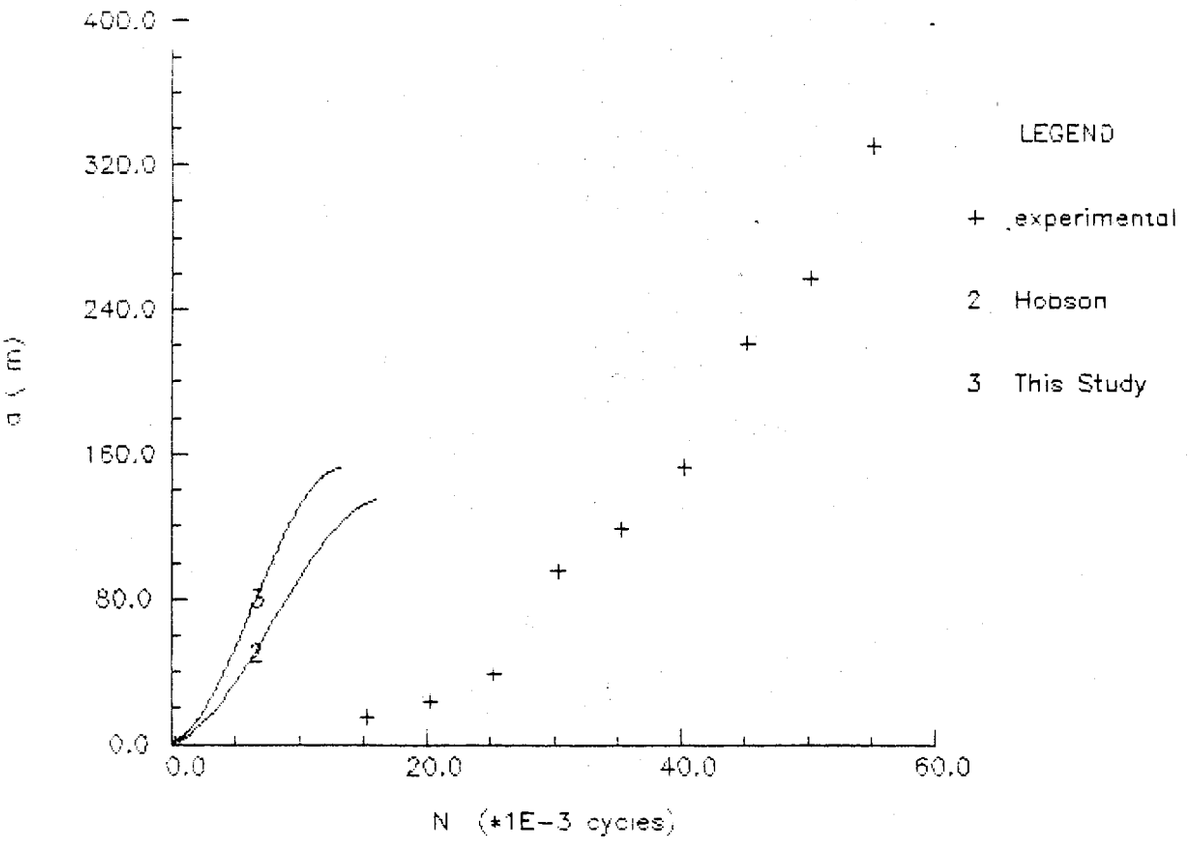

Figure 9. Plot of Model Approximations and Experimental Data for Specimen 4

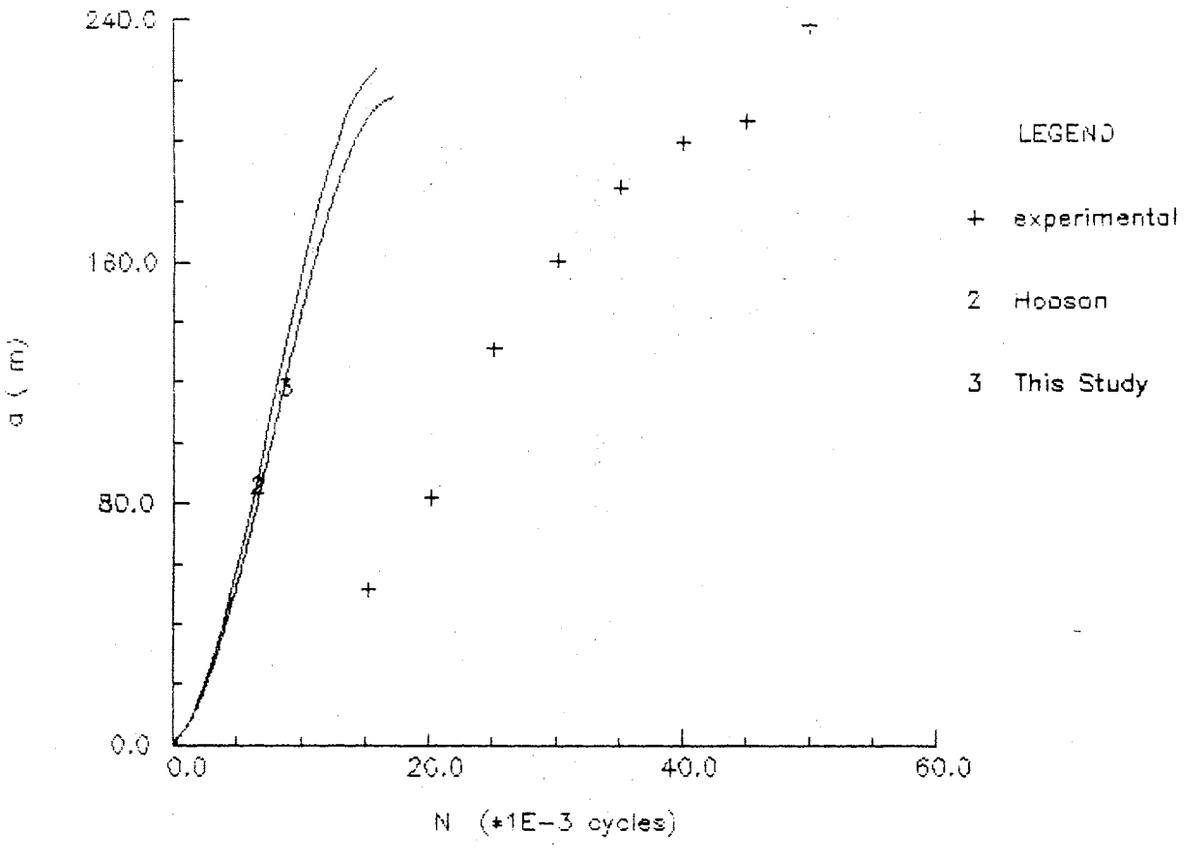

Figure 10. Plot of Model Approximations and Experimental Data for Specimen 5

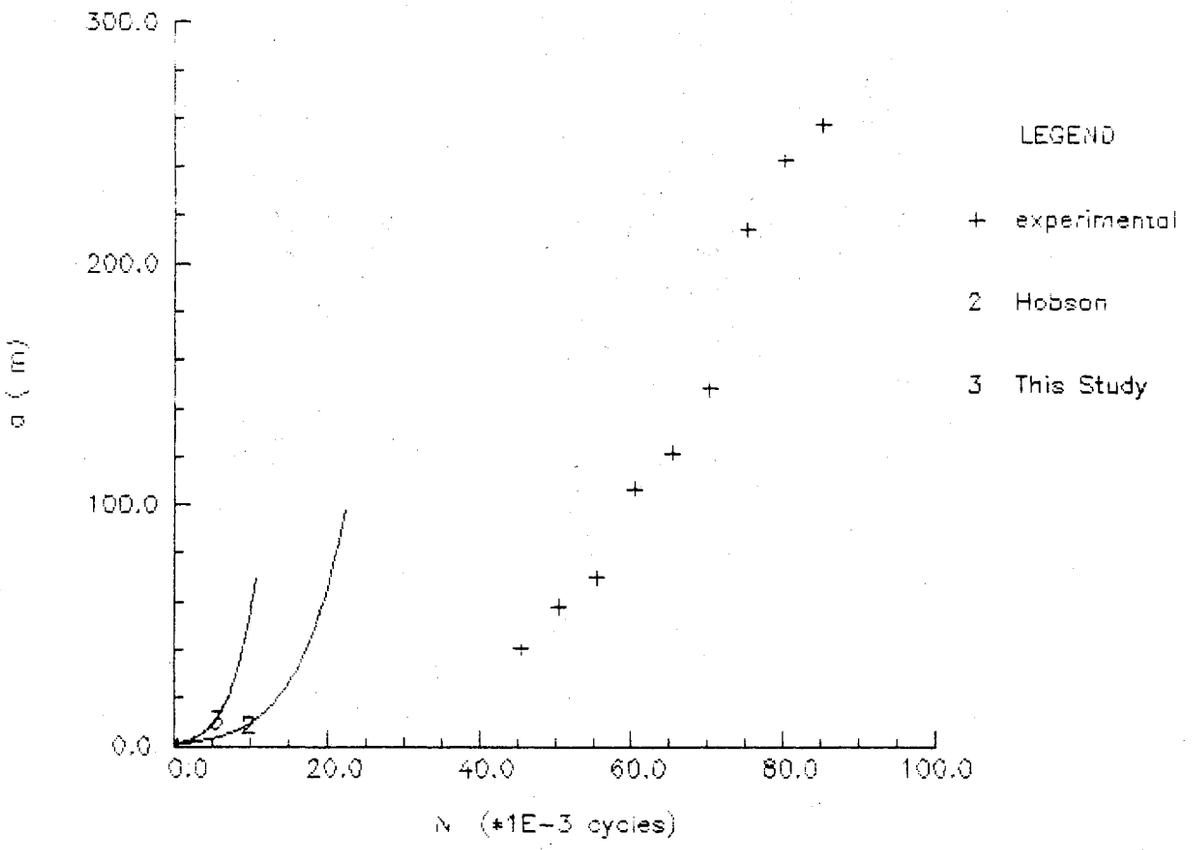

Figure 11. Plot of Model Approximations and Experimental Data for Specimen 6

of initiation was not known, the curves were translated horizontally, keeping the initiation point the same for both curves, until the curves best fit the experimental data. Upon visual inspection, the curve best matching the data is taken to be the better approximation.

The results showed that the modified technique of applying the model, in general, improved the accuracy somewhat. For specimens 1 and 2, the technique presented in this paper clearly improved the results of the model. For specimen 5, the two techniques provided very similar results; however, the technique presented here provided a slightly better result. For specimens 3 and 4, the results, again, were similar; however, Hobson's technique proved to be slightly better. As was feared, neither technique provided a good approximation for specimen 6. For this specimen, neither technique can be judged better.

CHAPTER V

SUMMARY AND CONCLUSIONS

Researchers are just beginning to study the growth of short fatigue cracks. Few original models have been developed to simulate this phenomenon. Of those proposed, their application is often complex. Simplification of their application can reduce the quality of the model. This was the case in Hobson's 1986 application of his own model proposed in 1982. This thesis examined the model and the recommended technique of application and proposed modifications and enhancements to both the model and its application in an effort to improve the model.

For the specimens examined, the new technique shows some improvement over the original model and application technique prescribed by Hobson; however, the improvement is, in general, significant yet somewhat costly. One must ultimately decide whether the improvement of the model justifies the additional effort required. This justification must be made on an individual basis, considering the need for improved accuracy and the availability of accurate data.

As an aside, it is interesting to note that neither technique showed a prejudice toward specimen type. In addition, from the data gathered here, while specimen

orientation significantly affected Stage II growth and fractography, there is no conclusive evidence that the specimen orientation plays a significant role in the short fatigue crack growth. It deduced that if stringers are the only microstructural feature making the material isotropic, they could greatly affect the crack growth behavior of long cracks while not affecting short crack growth. This is subject to the provision that the stringers are located sufficiently far from the point of crack initiation. It is believed that this was the case in this study.

One of the remaining questions concerns the specimens showing multiple growth retardations prior to long crack growth behavior. It would be interesting to determine whether or not these subsequent retardations are the result of short crack growth behavior re-emerging following the initial retardation. There was also inconclusive evidence suggesting a single microstructural feature that determines the value of d. If this feature could be pin-pointed, the study of short crack growth behavior could advance with a much higher level of certainty and confidence.

REFERENCES

Shigley, J. E. and Mishke, C. R. (1988) Mechanical Engineering Design (5th Ed.). McGraw-Hill Book Company. New York.

Gallagher, J. P., et al. (1984) USAF Damage Tolerant Design Handbook: Guidelines for the Analysis and Design of Damage Tolerant Aircraft Structures. University of Dayton Research Institute. Dayton, Ohio.

Hobson, P. D. (1982) The Formulation of a Crack Growth Equation for Short Cracks. Fatigue of Engineering Materials and Structures, Vol. 5, pp. 323-327.

Hobson, P. D., et al. (1986) Two Phases of Short Crack Growth in a Medium Carbon Steel. The Behaviour of Short Fatigue Cracks. Edited by K. J. Miller and E. R. de los Rios. Mechanical Engineering Publications Limited. London.

Radhakrishnan, V. M. and Mutoh, Y. (1986) On Fatigue Crack Growth in Stage I. The Behaviour of Short Fatigue Cracks. Edited by K. J. Miller and E. R. de los Rios. Mechanical Engineering Publications Limited. London.

Hertzberg, R. W. (1983) Deformation and Fracture Mechanics of Engineering Materials (2nd Ed.). John Wiley and Sons. New York.

The International Nickel Company, Inc. (1966) Huntington Alloy Products Division Technical Bulletin T-42: Engineering Properties of Inconel Alloy 625. Huntington, West Virginia.

Gerald, C. F. and Wheatley, P. O. (1985) Applied Numerical Analysis (3rd Ed.). Addison-Wesley Publishing Company. Reading, Massachusetts.

APPENDIXES

APPENDIX A

EXPERIMENTAL DATA

Experimental Data -- Specimen 1

Specimen Type -- T-L

D = 1.05 mm ρ = 0.20 mm

N (thousands)	a (μm)
75	42.5
85	45.0
100	55.0
115	70.0
130	112.5
150	157.5
170	190.0
190	233.3
210	270.0
230	325.0
250	365.0
270	435.0
290	455.0
320	518.3
350	635.3
380	813.3
410	1030.0

Experimental Data -- Specimen 2

Specimen Type -- L-T

D = 1.00 mm ρ = 0.20 mm

N (thousands)	a (μm)
25	16.5
50	35.5
75	47.5
100	73.0
125	92.0
150	128.5
175	154.5
200	192.5
225	221.0
250	253.0
275	264.2
325	293.5
350	373.5
450	575.0
500	811.5
550	996.5
600	1140.0
650	1720.0
700	3530.0

Experimental Data -- Specimen 3

Specimen Type -- T-L

D = 1.63 mm ρ = 0.20 mm

N (thousands)	a (μm)
15.21	11.8
22.72	18.8
27.75	50.6
30.76	60.0
33.27	64.7
38.27	72.0
43.27	98.8
48.27	101.2
53.30	114.6
58.31	153.7

Experimental Data -- Specimen 4

Specimen Type -- L-T

D = 1.63 mm ρ = 0.20 mm

N (thousands)	a (μm)
15	15.3
20	24.7
25	40.0
30	96.5
35	119.5
40	153.7
45	222.0
50	258.5
55	331.7
60	400.0

Experimental Data -- Specimen 5

Specimen Type -- T-L

D = 1.87 mm ρ = 0.19 mm

N (thousands)	a (μm)
15	51.8
20	82.4
25	131.7
30	161.0
35	185.4
40	200.0
45	207.3
50	239.0

Experimental Data -- Specimen 6

Specimen Type -- L-T

D = 1.54 mm ρ = 0.21 mm

N (thousands)	a (μm)
45	41.5
50	58.5
55	70.7
60	107.3
65	122.0
70	148.8
75	214.6
80	243.9
85	258.5

APPENDIX B

SECANT DATA

Secant Data -- Specimen 1

	a' (μm)	da/dN (*10^{-10} m/cycle)
*	21.3	5.7
*	43.8	2.5
	50.0	6.7
	62.5	10.0
o	91.3	28.3
o	135.0	22.5
o	173.8	16.3
	211.7	21.7

* Indicates points used to calculate a value of d via Hobson's technique.

o Indicates points which could be used to calculate an alternate value of d via Hobson's technique.

Secant Data -- Specimen 2

	a' (μm)	da/dN (*10^{-10} m/cycle)
	8.3	6.6
*	26.0	7.6
*	41.5	4.8
o	60.3	10.2
o	82.5	7.6
	110.3	14.6
	141.5	10.4
•	173.5	15.2
•	206.8	11.4
•	237.0	4.5
•	258.6	4.5
	278.9	5.9
	333.5	32.0

* Indicates points used to calculate a value of d via Hobson's technique.

o Indicates points which could be used to calculate an alternate value of d via Hobson's technique.

• Indicates points which could be used to calculate another alternate value of d via Hobson's technique.

Secant Data -- Specimen 3

	a' (μm)	da/dN (*10^{-10} m/cycle)
	5.9	7.8
	15.3	9.3
*	34.7	63.2
*	55.3	31.2
*	62.4	18.7
*	68.4	14.6
	85.4	53.6

* Indicates points used to calculate a value of d via Hobson's technique.

Secant Data -- Specimen 4

	a' (μm)	da/dN (*10^{-10} m/cycle)
	7.7	10.2
	20.0	18.8
	32.4	30.6
*	68.3	113.0
*	108.0	46.0
	136.6	68.4

* Indicates points used to calculate a value of d via Hobson's technique.

Secant Data -- Specimen 5

	a' (μm)	da/dN (*10^{-10} m/cycle)
	25.9	34.5
	67.1	61.2
*	107.1	98.6
*	146.4	58.6
*	173.2	48.8
*	192.7	29.2
*	203.7	14.6
	223.2	63.4

* Indicates points used to calculate a value of d via Hobson's technique.

Secant Data -- Specimen 6

	a' (μm)	da/dN (*10^{-10} m/cycle)
	20.8	9.2
*	50.0	34.0
*	64.6	24.4
o	89.0	73.2
o	114.7	29.4
	135.4	53.6

* Indicates points used to calculate a value of d via Hobson's technique.

o Indicates points which could be used to calculate an alternate value of d via Hobson's technique.

APPENDIX C

FITTED CURVES

Specimen 1

Curve 1 is good from 0.0000< (N/1000) <115.0000.
The coefficients for curves relating to range 1 are:

a		da/dN	
a0 =	4.35368660255335E-0002	a0 =	1.07860305900249E+0000
a1 =	1.07860305900249E+0000	a1 =	-1.73534427307800E-0002
a2 =	-8.67672136538999E-0003	a2 =	-2.50159896907354E-0005
a3 =	-8.33866323024512E-0006	a3 =	1.67784764255538E-0006
a4 =	4.19461910638845E-0007		

variance = 0.00000000000000E+0000

Specimen 2

Curve 1 is good from 0.0000< (N/1000) <100.0000.
The coefficients for curves relating to range 1 are:

a		da/dN	
a0 =	-4.56765386043116E-0001	a0 =	7.19972423251420E-0001
a1 =	7.19972423251420E-0001	a1 =	6.54998290798403E-0003
a2 =	3.27499145399202E-0003	a2 =	-3.85209064986292E-0004
a3 =	-1.28403021662171E-0004	a3 =	3.87657133074648E-0006
a4 =	9.69142832686620E-0007		

variance = 0.00000000000000E+0000

Specimen 3

Curve 1 is good from 22.7200< (N/1000) <43.2700.
The coefficients for curves relating to range 1 are:

a		da/dN	
a0	= -1.97837147174403E+0002	a0	= 1.22385524562415E+0001
a1	= 1.22385524562415E+0001	a1	= -6.09227434979402E-0002
a2	= -3.04613717489701E-0002	a2	= -1.05739152826345E-0002
a3	= -3.52463842754602E-0003	a3	= -1.49196712848632E-0004
a4	= -3.72991782121579E-0005	a4	= 7.85894193917891E-0006
a5	= 1.57178838783821E-0006		

variance = 0.00000000000000E+0000

Specimen 4

Curve 1 is good from 25.0000< (N/1000) <40.0000.
The coefficients for curves relating to range 1 are:

a	da/dN
a0 = -2.23019646690693E+0002	a0 = 1.04186977297068E+0001
a1 = 1.04186977297068E+0001	a1 = 1.42525479250480E-0001
a2 = 7.12627396252401E-0002	a2 = -7.27516530033512E-0003
a3 = -2.42505510011171E-0003	

variance = 0.00000000000000E+0000

Specimen 5

Curve 1 is good from 20.0000< (N/1000) <50.0000.
The coefficients for curves relating to range 1 are:

a		da/dN	
a0 =	-1.75210585939232E+0002	a0 =	1.68117060106306E+0001
a1 =	1.68117060106306E+0001	a1 =	-2.83563336165116E-0001
a2 =	-1.41781668082558E-0001	a2 =	-9.13852455460074E-0003
a3 =	-3.04617485153713E-0003	a3 =	1.94691740611264E-0004
a4 =	4.86729351528159E-0005		

variance = 8.05634252751479E+0001

Specimen 6

a

a0 = -357.2
a1 = 13.72
a2 = -0.1080

APPENDIX D

GENERATED STRESS INTENSITY RANGE AND C DATA

Calculated Data -- Specimen 1

a (μm)	delta K (MPa√m)	C (1/cycles)
3.54	1.5770	0.054895
6.84	2.1920	0.046092
9.95	2.6436	0.041903
12.87	3.0065	0.039357
15.60	3.3099	0.037634
18.14	3.5690	0.036404
20.50	3.7940	0.035512
22.68	3.9905	0.034881
24.70	4.1643	0.034478
26.56	4.3181	0.034306
28.27	4.4549	0.034396
29.84	4.5768	0.034818
31.28	4.6859	0.035696
32.62	4.7851	0.037241
33.85	4.8744	0.039823
35.01	4.9571	0.044147
36.10	5.0337	0.051743
37.15	5.1063	0.066788
38.17	5.1758	0.107402
39.19	5.2445	4.279800

Calculated Data -- Specimen 2

a (μm)	delta K (MPa√m)	C (1/cycles)
1.91	1.1455	0.066538
4.33	1.7247	0.049385
6.76	2.1549	0.042624
9.20	2.5138	0.038831
11.62	2.8251	0.036366
14.02	3.1030	0.034641
16.37	3.3529	0.033392
18.66	3.5796	0.032492
20.90	3.7883	0.031879
23.07	3.9800	0.031534
25.18	4.1579	0.031468
27.23	4.3237	0.031725
29.21	4.4780	0.032386
31.14	4.6235	0.033587
33.02	4.7609	0.035564
34.87	4.8923	0.038751
36.69	5.0183	0.044038
38.51	5.1411	0.053666
40.35	5.2624	0.075968
42.22	5.3828	0.244640

Calculated Data -- Specimen 3

a (μm)	delta K (MPa√m)	C (1/cycles)
26.49	4.7736	0.165189
30.06	5.0848	0.151245
33.46	5.3645	0.140005
36.68	5.6165	0.130723
39.74	5.8458	0.122931
42.64	6.0552	0.116328
45.39	6.2472	0.110717
47.99	6.4234	0.105976
50.44	6.5852	0.102041
52.77	6.7354	0.098892
54.98	6.8749	0.096558
57.07	7.0042	0.095121
59.07	7.1257	0.094729
60.98	7.2399	0.095637
62.82	7.3482	0.098272
64.60	7.4514	0.103406
66.34	7.5510	0.112595
68.05	7.6476	0.129668
69.76	7.7430	0.168567
71.48	7.8377	0.525155

Calculated Data -- Specimen 4

a (μm)	delta K (MPa√m)	C (1/cycles)
51.06	6.6255	0.129014
57.90	7.0549	0.122991
64.60	7.4514	0.118270
71.16	7.8202	0.114543
77.58	8.1649	0.111609
83.84	8.4876	0.109338
89.95	8.7911	0.107645
95.88	9.0759	0.106482
101.65	9.3448	0.105830
107.24	9.5981	0.105700
112.65	9.8370	0.106135
117.87	10.0622	0.107222
122.89	10.2741	0.109113
127.72	10.4739	0.112065
132.33	10.6612	0.116528
136.73	10.8369	0.123345
140.92	11.0017	0.134290
144.88	11.1552	0.153900
148.60	11.2975	0.199210
152.09	11.4295	0.566159

Calculated Data -- Specimen 5

a (μm)	delta K (MPa√m)	C (1/cycles)
98.22	9.5998	0.079772
108.13	10.0720	0.075258
117.47	10.4977	0.071410
126.25	10.8827	0.068079
134.50	11.2325	0.065168
142.23	11.5507	0.062615
149.47	11.8411	0.060384
156.23	12.1060	0.058457
162.54	12.3482	0.056837
168.44	12.5704	0.055548
173.95	12.7746	0.054634
179.11	12.9629	0.054168
183.96	13.1375	0.054264
188.52	13.2996	0.055099
192.84	13.4515	0.056957
196.97	13.5950	0.060325
200.95	13.7320	0.066133
204.83	13.8643	0.076474
208.65	13.9934	0.097678
212.48	14.1216	0.168950

Calculated Data -- Specimen 6

a (μm)	delta K (MPa$\sqrt{m}$)	C (1/cycles)
43.45	5.9642	0.092740
45.35	6.0930	0.087153
47.20	6.2160	0.082076
49.00	6.3333	0.077438
50.74	6.4446	0.073181
52.43	6.5509	0.069256
54.06	6.6519	0.065624
55.65	6.7489	0.062252
57.18	6.8409	0.059110
58.65	6.9282	0.056177
60.08	7.0121	0.053434
61.45	7.0915	0.050865
62.77	7.1672	0.048460
64.03	7.2387	0.046215
65.25	7.3072	0.044130
66.41	7.3718	0.042218
67.51	7.4325	0.040519
68.57	7.4906	0.039130
69.57	7.5450	0.038376
70.51	7.5957	0.040982

VITA 2

Robert Glen Stone

Candidate for the Degree of

Master of Science

Thesis: A STUDY OF THE SHORT FATIGUE CRACK GROWTH CHARACTERISTICS OF INCONEL 625 BY MODIFICATION AND APPLICATION OF A SHORT FATIGUE CRACK GROWTH MODEL

Major Field: Mechanical Engineering

Biographical:

Personal Data: Born in Tulsa, Oklahoma, October 30, 1965, the son of Wm. Paul and Ilona Stone.

Education: Graduated from Union High School, Tulsa, Oklahoma, in May 1983; received Bachelor of Science Degree in Mechanical Engineering from Oklahoma State University in July, 1987; completed requirements for the Master of Science degree at Oklahoma State University in May, 1989.

Professional Experience: Teaching Assistant, Department of Mechanical and Aerospace Engineering, Oklahoma State University, June, 1987, to July, 1988; Engineering Intern with Texas Instruments, Dallas, Texas, Summers of 1985 and 1986.